Neuron, Vol. 26, 371–382, May, 2000, Copyright ©2000 by Cell Press

Drosophila Futsch Regulates Synaptic Microtubule Organization and Is Necessary for Synaptic Growth

Jack Roos,* Thomas Hummel,† Norman Ng,* Christian Klämbt,† and Graeme W. Davis*‡
*Dept. Biochemistry and Biophysics
Programs in Cell Biology and Neuroscience
University of California, San Francisco
San Francisco, California 94143
†Institut fuer Neurobiologie
Universitaet Muenster
Badestrasse 9
D-48149 Muenster
Germany

Summary

We present evidence that Futsch, a novel protein with MAP1B homology, controls synaptic growth at the *Drosophila* neuromuscular junction through the regulation of the synaptic microtubule cytoskeleton. Futsch colocalizes with microtubules and identifies cytoskeletal loops that traverse the lateral margin of select synaptic boutons. An apparent rearrangement of microtubule loop architecture occurs during bouton division, and a genetic analysis indicates that Futsch is necessary for this process. *futsch* mutations disrupt synaptic microtubule organization, reduce bouton number, and increase bouton size. These deficits can be partially rescued by neuronal overexpression of a *futsch* MAP1B homology domain. Finally, genetic manipulations that increase nerve-terminal branching correlate with increased synaptic microtubule loop formation, and both processes require normal Futsch function. These data suggest a common microtubule-based growth mechanism at the synapse and growth cone.

Introduction

The precise modification of nerve-terminal morphology is essential for the correct wiring and plasticity of neuronal circuitry. One mechanism for the addition of new synapses to a nerve terminal involves the sprouting of new synaptic boutons (Casadio et al., 1999; Engert and Bonhoeffer, 1999). Recently, at the *Drosophila* neuromuscular junction (NMJ), it has been suggested that one mechanism for nerve-terminal sprouting involves the division of preexisting synaptic boutons (Zito et al., 1999). These results further suggest that division of a synaptic bouton into thirds (or greater subdivisions) may be a mechanism for generating a branchpoint in the nerve terminal (Zito et al., 1999). Recent evidence suggests that in the hippocampus, synaptic morphological change is associated with the consolidation of long-term synaptic plasticity (Engert and Bonhoeffer, 1999; Toni et al., 1999). In particular, the sprouting of new postsynaptic spines that contact preexisting presynaptic boutons may be a mechanism for generating new synaptic contacts (Engert and Bonhoeffer, 1999; Toni et al., 1999).

Nerve-terminal plasticity achieved through processes such as nerve-terminal sprouting will require precisely controlled and spatially regulated modifications to the nerve-terminal cytoskeleton. The cytoskeletal rearrangements that drive bouton division and the signaling events that control this process are not known. In principle, localized remodeling of the cytoskeleton could achieve the spatial precision required for synapse-specific, activity-dependent plasticity (Grant et al., 1995; Halpain et al., 1998; Rohatgi et al., 1999; Wills et al., 1999a, 1999b). Specificity could be further refined if only a small subset of synapses, at any given time, has the capacity for cytoskeletal rearrangement.

The regulation of the neuronal cytoskeletal at the growth cone has been studied extensively (Tanaka and Sabry, 1995; Luo et al., 1997; Suter and Forscher, 1998; Gallo and Letourneau, 1999; Wills et al., 1999a, 1999b). Recently, it has been demonstrated that the regulation of microtubule organization within the growth cone may be an important determinant of growth cone motility. The macroscopic organization of microtubules within the growth cone is dynamic as revealed by the formation and destruction of hairpin loop structures that incorporate a large portion of the growth cone microtubules (Tanaka et al., 1991; Dent et al., 1999). Of particular interest is the demonstration that the formation of microtubule hairpin loops is correlated with the cessation of growth cone motility and the opening (or destruction) of these loops is correlated with the reestablishment of motility (Dent et al., 1999). These data are strengthened by the observation that the transition of a motile growth cone to a stable synaptic contact is also correlated with the formation of a hairpin microtubule loop within the growth cone as it transforms into a synapse (Tsui et al., 1984). Thus, regulated microtubule architecture appears to be an essential element in the control of growth cone morphology and motility as well as synapse formation. The molecular regulation of these microtubule based structures, however, is not known.

In the present study, we implicate a novel protein, Futsch, in the regulation of the synaptic microtubule cytoskeleton and provide genetic evidence that Futsch is necessary for synaptic growth. Hummel et al. (2000 [this issue of *Neuron*]) have identified Futsch as a novel *Drosophila* cytoskeletal-associated protein of 5327 amino acids that has homology with vertebrate MAP1B at the N and C termini. Futsch is associated with the dendritic, axonal, and nerve-terminal cytoskeleton. Futsch is shown to associate with microtubules in vitro, and a genetic analysis demonstrates that Futsch is necessary for axonal and dendritic growth. Here we demonstrate that Futsch colocalizes with microtubules and is necessary for the organization of synaptic microtubule cytoskeleton. We further demonstrate that Futsch is necessary for normal synaptic growth, implicating the synaptic microtubule cytoskeleton in this process.

Of particular interest, we identify microtubule hairpin loops within a small subset of synaptic boutons at the

‡To whom correspondence should be addressed (e-mail: gdavis@biochem.ucsf.edu).

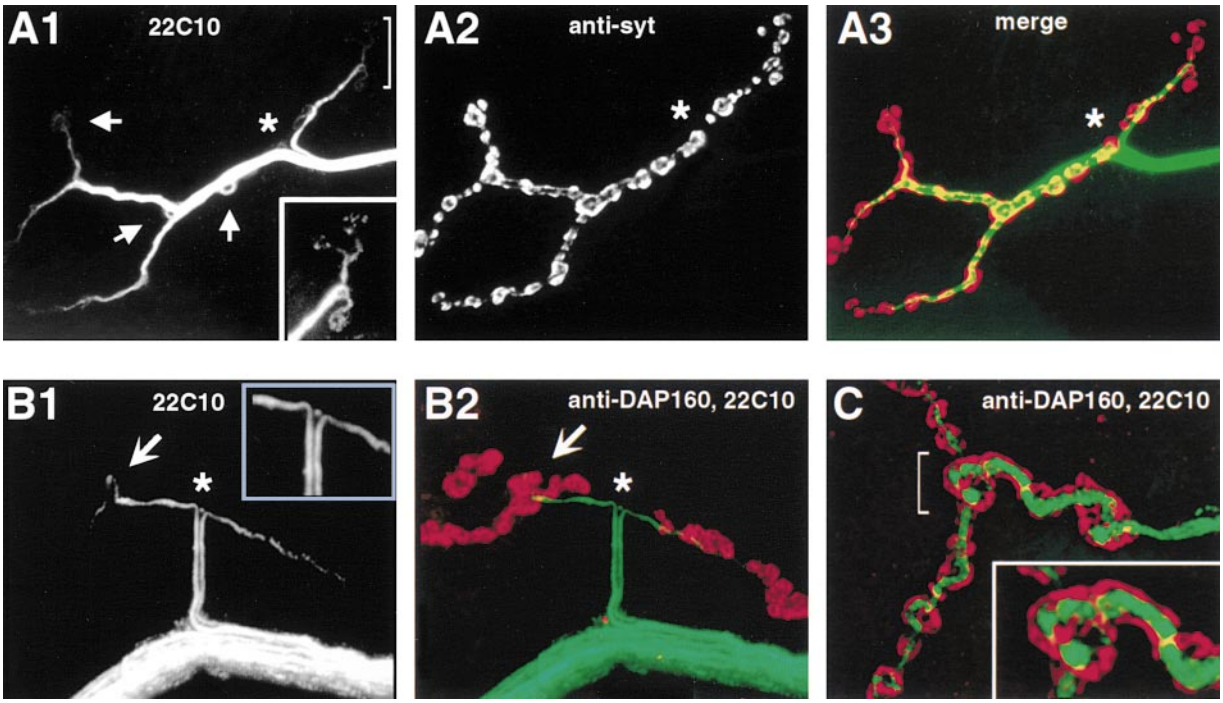

Figure 1. Loops of Futsch Immunoreactivity Are Observed within a Subset of Synaptic Boutons at Muscle 4

(A1) mAb 22C10 (anti-Futsch) reveals a core cytoskeleton within the axon that is continuous with the nerve terminal. Two type 1b axons innervate muscle 4 and arborize in opposite directions from the site of muscle contact (asterisk). Cytoskeletal loops identified by Futsch immunoreactivity (22C10) are observed at a subset of boutons (arrows) and are always observed at end-terminal boutons (see inset).

(A2) Antisynaptotagmin staining and the merged image (A3) show the position of Futsch loops within the terminal.

(B1) The two nerves innervating muscle 4 are stabilized on the muscle (inset) and extend on the muscle surface before boutons are elaborated.

(B2) Loops are only observed within synaptic boutons (arrow).

(C) mAb 22C10 (green) is localized close to but below the plasma membrane as defined by antibody staining for dynamin-associated protein (DAP160, red). The immunofluorescent image shown was deconvolved using Delta-Vision algorithms to eliminate out-of-plane fluorescent scatter.

Drosophila neuromuscular synapse. Synaptic microtubule loops are subsynaptic specializations that identify unique boutons within the *Drosophila* neuromuscular synapse. We provide evidence that synaptic microtubule loops are stabilized by Futsch. We provide further evidence that loops are associated with stable synaptic boutons, while the dispersion or destruction of these loops is associated with boutons undergoing division or sprouting. These synaptic microtubule loops are highly reminiscent of microtubule loops present within the growth cone, implying a fundamental similarity between the mechanisms of growth cone motility and the mechanisms of synaptic growth and branching.

Results

Futsch Identifies Unique Cytoskeletal Structures at Select Synaptic Boutons

At the *Drosophila* NMJ, Futsch protein is associated with a cytoskeletal core within the synaptic terminal that is continuous with the axonal cytoskeleton. This cytoskeletal core is composed of multiple fibers, consistent with Futsch binding the microtubule cytoskeleton of the axon and nerve terminal (Figures 1A and 1B). Futsch is localized close to but below the nerve-terminal plasma membrane. Synaptic terminals double stained for Futsch and the synaptic plasma membrane protein DAP160 (dynamin-associated protein 160; Roos and Kelly, 1999) do not show overlapping staining. Rather, Futsch is a discrete core of staining just inside the plasma membrane as defined by DAP160 (Figure 1C). Further evidence that Futsch colocalizes with microtubules is presented below.

Examination of Futsch staining at the nerve terminal using deconvolution confocal microscopy reveals periodic loop structures within a subset of synaptic boutons (loops are present within 24% $\pm$ 3% of boutons at the wild-type synapse on muscles 6 and 7 and 22% $\pm$ 3% of boutons at muscle 4; Figures 1A and 1B, arrows). These loops appear at stereotypic locations within the synapse at every abdominal muscle, though for the purpose of visualization, we have focused our analysis on muscle 4. Futsch-positive loops are present within all types of synaptic boutons, including type 1b, type 1s, and type II (see Keshishian et al., 1996 for bouton-type definition). We have restricted our analysis to type 1b boutons.

Synaptic microtubule loops are highly enriched at points of nerve-terminal branching ($\sim$90% of observed branchpoints include a loop), and loops are always present within the terminal bouton(s) at the end of each chain of synaptic boutons (Figure 1A, arrows and inset). The

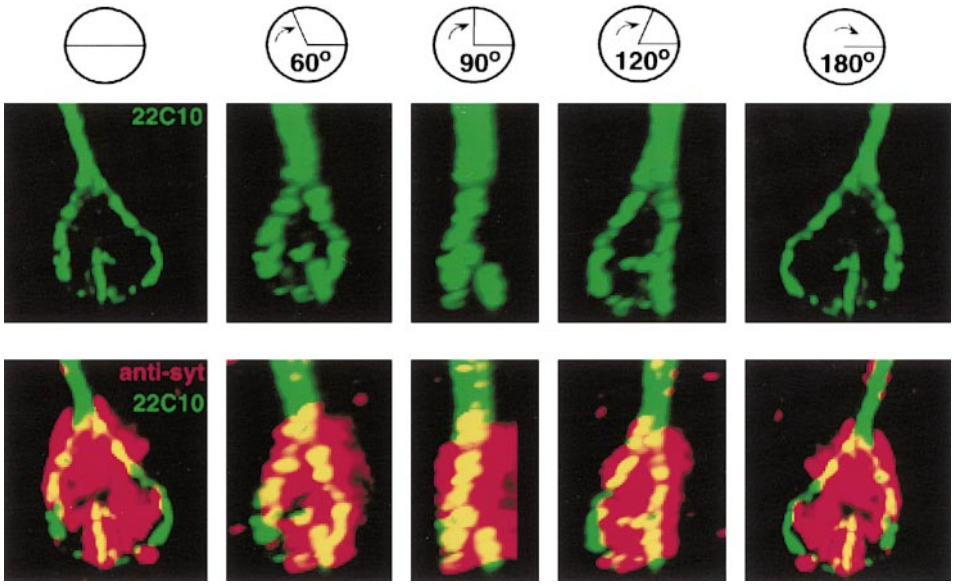

Figure 2. Three-Dimensional Reconstruction and Rotation of a Futsch/Microtubule Loop within a Single Synaptic Bouton

A single bouton is shown stained for Futsch (mAb 22C10) and antisynaptotagmin to delineate the boundary of the bouton. Following serial reconstruction the bouton is rotated around the y axis. The extent of rotation is indicated at the top of each pair of panels. The Futsch-positive cytoskeletal loop is entirely contained within the z axis of the synaptic bouton (panel 3; z axis is horizontal), demonstrating that the loop is not an artifact of confocal sectioning through a spherical structure. Images at the top and bottom of the z axis (panels 1 and 5) demonstrate that the loop traverses the widest diameter of the bouton, being closer to the plasma membrane than the diffuse antisynaptotagmin staining in some areas.

absence of loops at some branchpoints may reflect our inability to visualize these structures perfectly within every synapse. Microtubule loops are not present at the sites of muscle innervation where the axon initiates contact with the muscle surface. In Figures 1A and 1B, two axons, both originating from the segmental nerve, form type 1b terminals at muscle 4. These axons reach muscle 4 and migrate on the muscle surface in opposite directions (Figures 1A and 1B; an asterisk marks the site where these two axons separate on the muscle surface). The site of innervation is not a branchpoint but rather is the site of muscle innervation, and no loops are present. This morphology was consistently observed.

Cytoskeletal Loops Define the Lateral Margin of Select Synaptic Boutons

3D reconstructions of synaptic boutons that contain Futsch-positive loops, double stained with antisynaptotagmin (anti-syt; vesicle protein) to delineate the boundary of the synaptic bouton, demonstrate that these structures are indeed loops rather than an artifact of confocal sectioning through a spherical structure (Figure 2). Nerve terminals were double stained for anti-Futsch (22C10) and anti-syt, and optical sections were taken through the z plane of the nerve terminal of muscle 4 at 0.1 μm sections. Select synaptic boutons containing loop structures were serially reconstructed using DeltaVision deconvolution algorithms. Following reconstruction, loop-containing synaptic boutons can be rotated in three dimensions, demonstrating that the Futsch staining is a loop that traverses the widest diameter of the synaptic bouton and is entirely contained within the top and bottom (z plane) boundaries of the bouton as defined by synaptotagmin staining. Futsch-positive loops often extend beyond the anti-syt staining in the x and y dimension, indicating that the loop is closer to the plasma membrane than are diffuse synaptic vesicles in some areas of the bouton.

Microtubules Are Present within Synaptic Cytoskeletal Loops

We have followed the localization of microtubules at the third instar synapse by visualizing tubulin (antitubulin immunoreactivity) or by following the localization of neuronally overexpressed tau-GFP (Callahan and Thomas, 1994; Ito et al., 1997). Futsch colocalizes with synaptic microtubules as identified by anti-α-tubulin (Figure 3A). Colocalization is observed throughout the axon and synapse and always occurs at microtubule loops. Near perfect colocalization of Futsch and tubulin persists even when the microtubule organization is disrupted in hypomorphic Futsch mutations (see below), implying an association of Futsch with the microtubules (Figure 3B). Note that there is no immunoreactivity of Futsch with muscle microtubules, demonstrating that there is not antibody cross-reactivity in these double-staining experiments. Overexpressed tau-GFP also colocalizes with Futsch in synaptic cytoskeletal loop structures (Figure 3C, arrows). Tau-GFP appears more diffuse in some areas than anti-Futsch (22C10). However, the same qualitative difference is observed in the axon, and we believe that this is an artifact of tau-GFP overexpression. These data are consistent with Futsch being associated with the microtubule cytoskeleton as suggested by in vitro data (Hummel et al., 2000).

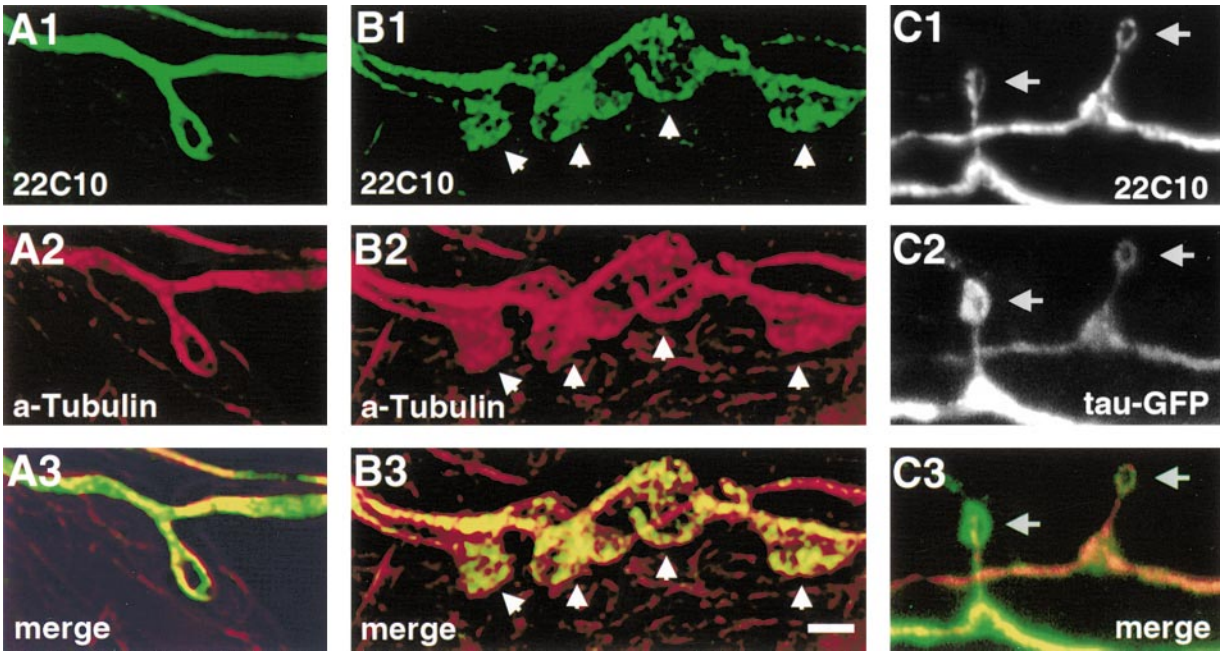

Figure 3. Futsch Colocalizes with Microtubules

(A) Colocalization of anti-Futsch (22C10; A1, green) and anti-α-tubulin (A2, red) at a synaptic terminal. In the merged image (A3, merge), note that muscle microtubules do not show 22C10 immunoreactivity, demonstrating the specificity of antibody staining.

(B) Colocalization of anti-Futsch (22C10; B1, green) and α-tubulin (red) persist in the *futsch*^{N94} hypomorphic mutant synapse despite the disorganization of the synaptic microtubule cytoskeleton. An arrowhead indicates each synaptic bouton.

(C) A synaptic terminal is shown that has been stained for anti-Futsch (22C10; C1) and that also contains overexpressed tau-GFP (*UAS-tau-GFP; elaV-GAL4* larval genotype; C2). These two proteins colocalize (merge) within synaptic loop structures (arrows) at the synapse (tau-GFP is green). Every synaptic cytoskeletal loop that was observed showed colocalization of anti-Futsch and tau-GFP.

Futsch Is Necessary for Microtubule Organization and Synaptic Growth

Two homozygous viable mutations in *futsch* were identified by Hummel et al. (2000). Both mutations alter synaptic growth (Figure 4). There is no detectable Futsch immunoreactivity in the *futsch*^{K68} mutation. *futsch*^{N94} is a hypomorphic mutation that reduces protein expression to ~20% wild-type levels (based on reduced fluorescence intensity). The *futsch*^{N94} mutation also disrupts the subcellular localization of Futsch. In *futsch*^{N94}, Futsch immunoreactivity fills up the volume of every synaptic bouton rather than being restricted to a cytoskeletal core (Figure 4C). Microtubule localization is also disrupted in these *futsch* mutations. In both *futsch*^{N94} and *futsch*^{K68}, synaptic microtubules no longer form a filamentous cytoskeletal shaft that runs through the nerve terminal, and microtubule loop formation is absent (Figure 4F and 4G). Rather, tubulin staining in these mutants is punctate and diffuse, filling up the volume of every synaptic bouton within the NMJ (Figures 4F and 4G). The diffuse, punctate tubulin staining in these mutants is identical to the diffuse anti-Futsch (22C10) staining observed in *futsch*^{N94} (Figure 4; compare [C] with [F] and [G]). Double staining for Futsch and α-tubulin demonstrates that colocalization persists even when the microtubules are dispersed in these mutations (Figure 3B). Finally, there is a qualitative disruption of both anti-Futsch and tubulin staining in *futsch*^{N94}/+ heterozygous larvae; microtubule loops are not as clearly defined at the lateral margin of select synaptic boutons (data not shown). Taken together, these data demonstrate that *futsch* is necessary for microtubule organization within synaptic boutons. These data also support the conclusion that *futsch* is necessary for the formation or stabilization of microtubule-based loop structures.

Synaptic morphology is severely altered in viable *futsch* mutant backgrounds, indicating that Futsch-dependent microtubule organization is necessary for normal synaptic growth and development (Figure 4). In *futsch*^{N94} and *futsch*^{K68}, there is a reduction in bouton number and an increase in bouton size (Figures 4B and 4C). Bouton number is reduced from an average of 64.8 (±4.1) boutons at muscle 4 in wild type to 37.9 (±3.5) in *futsch*^{N94} and 40.8 (±3.2) in *futsch*^{K68} ($p < 0.001$). We do not observe a change in muscle size in these mutations. There is also a modest but statistically significant reduction in bouton number in *futsch*^{N94}/+ heterozygous larvae (51.2 ± 3.3 boutons at muscle 4; $p < 0.01$). This correlates with a qualitative disruption in microtubule organization at the NMJ in these heterozygous larvae (described above). In parallel with the observed decrease in bouton number, we observed that the average bouton size and the distribution of bouton sizes within the synapse are dramatically increased in both *futsch* alleles (Figure 4H; see legend for average bouton sizes). Mutant nerve-terminals at muscle 4 rarely have branchpoints. However, this may be a consequence of the drastic reduction in bouton number.

Genetic rescue experiments demonstrate that *futsch*

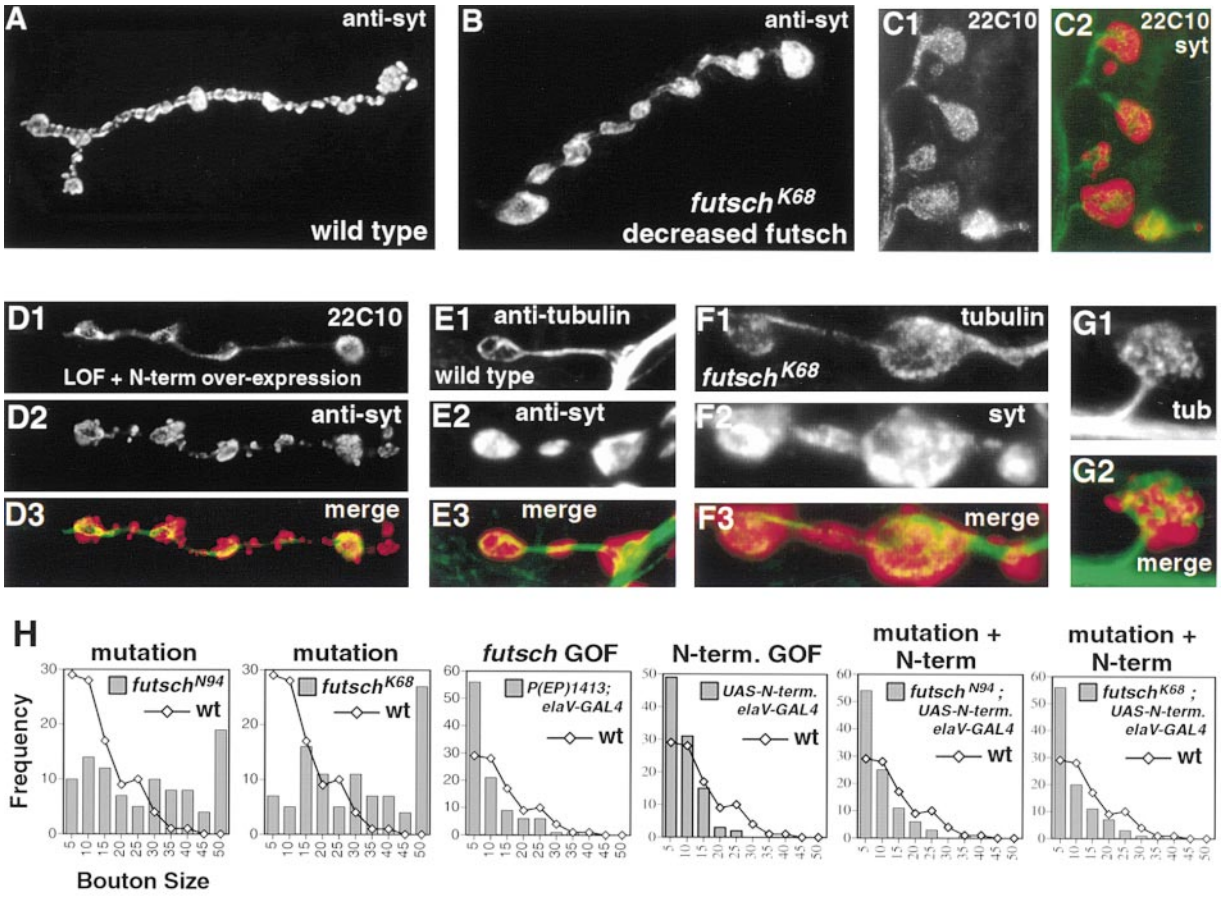

Figure 4. Futsch Is Necessary for Normal Synaptic Growth and Development

(A) The wild-type synapse at muscle 4 is shown stained with antisynaptotagmin.

(B) The synapse on muscle 4 is shown in the *futsch*^{K68} mutation that eliminates *futsch* protein as detected by mAb 22C10 immunoreactivity. Synaptic boutons are fewer and larger.

(C) Select synaptic boutons are shown at muscle 4 in the *futsch*^{N94} mutation that significantly reduces mAb 22C10 staining (C1; exposure time is ~20× longer for these images compared to all other mAb 22C10 images presented in the manuscript). The mAb 22C10 staining is mislocalized in *futsch*^{N94}, being distributed throughout every bouton (C2; merged image of anti-Futsch in green with antisynaptotagmin in red to delineate the synaptic bouton).

(D) Image of the synapse at muscle 4 in *futsch*^{N94} with overexpression of N-terminal Futsch (LOF + N-term overexpression) in all neurons (driven by *elaV-GAL4*). Anti-DAP160 is shown in red, anti-Futsch in green.

(E) Anti-α-tubulin identifies microtubule loops within synaptic boutons of a wild-type terminal. An end-terminal loop is revealed at the end of a chain of synaptic boutons.

(F and G) Tubulin staining is mislocalized in the *futsch*^{K68} mutation (F) and *futsch*^{N94} (G), appearing punctate and diffusing to fill the volume of every synaptic bouton.

(H) Quantification of bouton size is shown based on measurement of the longest bouton dimension multiplied by the perpendicular planar axis. A line indicating the wild-type size distribution is superimposed on each graph. Shown are bouton sizes measured at synapses in the *futsch* homozygous–viable mutants *futsch*^{K68} and *futsch*^{N94} (mutation) at synapses overexpressing full-length Futsch in all nerves (*futsch* GOF; ep(X)1419; *elaV-GAL4*) and at mutant synapses that also overexpress the *futsch* N-terminal microtubule binding domain (mutant + N-term). Bouton sizes with areas larger than 50 μm^2 are grouped in a single bin. Average bouton sizes for each genotype are as follows: wild type = 9.1 μm^2, *futsch*^{N94} = 22.2 μm^2, *futsch*^{K68} = 26.8 μm^2, P(EP)1419/*elaV-GAL4* = 7.1 μm^2, *UAS-Nterm/elaV-GAL4* = 6.4 μm^2, *futsch*^{N94}*; UAS-Nterm/elaV-GAL4* = 6.4 μm^2, *futsch*^{K68}*; UAS-Nterm/elaV-GAL4* = 6.8 μm^2.

(A)–(D) are the same magnification. (E)–(G) are each at the same magnification (~2× magnification compared to that shown for [A]–[D]).

loss-of-function is responsible for the observed disruption in microtubule organization and is responsible for the observed deficits in synaptic growth and development. We are able to achieve a partial rescue of the *futsch* mutant phenotype by overexpression of the N-terminal, predicted microtubule-binding domain of Futsch (Hummel et al., 2000). At present, a full-length cDNA is not available for the large 5327 amino acid transcript. Overexpression of the *UAS-Nterminal-Futsch* construct in the *futsch*^{N94} and *futsch*^{K68} mutant backgrounds reverted the mutant phenotype to nearly wild type (Figure 4D). Bouton numbers were increased from an average of 37.9 (±3.5) in *futsch*^{N94} to an average of 51.4 (±3.6) in *futsch*^{N94} larvae that also overexpress the N-terminal construct neuronally (*futsch*^{N94}*; UASN-term/+; elaV-GAL4*). In *futsch*^{K68}, bouton number was increased from 40.9 (±3.2) to 52.3 (±2.9) by the N-terminal rescue ($p < 0.01$). Thus, average bouton numbers are partially

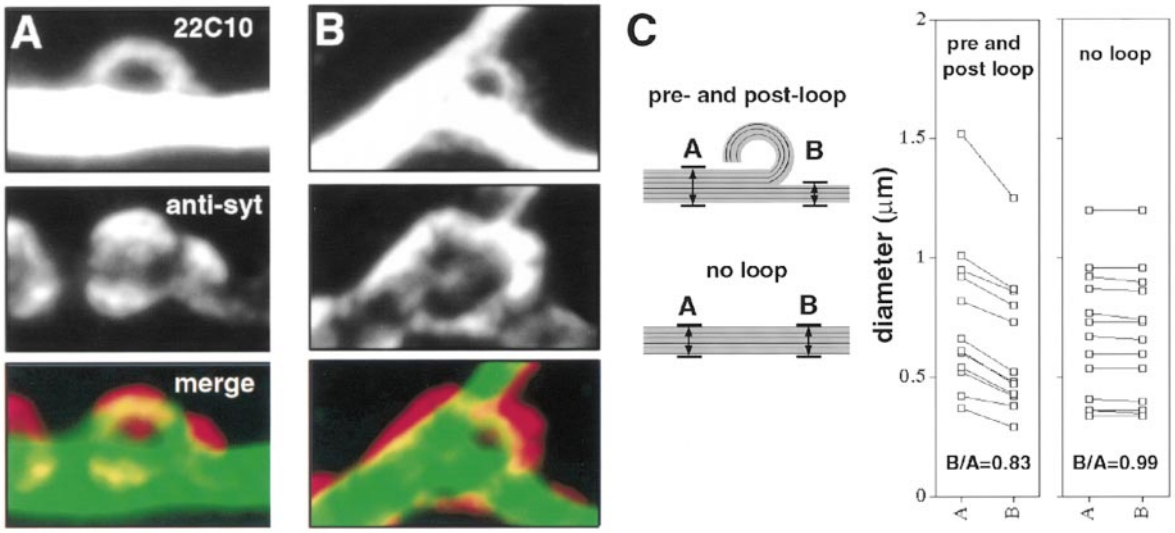

Figure 5. Microtubules within a Loop Do Not Rejoin the Major Nerve-Terminal Cytoskeletal Shaft

(A) High magnification view of an individual synaptic loop showing both mAb 22C10 and antisynaptotagmin (anti-syt) and the merged image (22C10 in green and synaptotagmin in red).

(B) Staining identical to that shown in (A), showing a loop present at a nerve-terminal branchpoint.

(C) Measurements of the diameter of mAb 22C10 staining in the nerve-terminal shaft were taken 0.5 μm before (A) and 0.5 μm after (B) loops at various positions within the NMJ (pre- and post-loop). Alternatively, measurements were taken at two sites (A and B) separated by 4 μm (larger than the average loop diameter) at various positions along the NMJ without an interposed loop (no loop). The diameter of the 22C10-positive cytoskeletal shaft is consistently and significantly reduced following a Futsch-positive loop (pre- and post-loop) compared to the normal attenuation of the cytoskeleton without an interposed loop (no loop). The calculated ratio of measurements taken from site A and site B are shown at the bottom of the graph.

rescued by N-terminal overexpression [wild-type bouton number = 64.8 (±4/1)], although there remain statistically fewer boutons in the rescues compared to wild type ($p < 0.01$).

The abnormally large average bouton size observed in the *futsch* mutants is also rescued by overexpression of the N terminus in the mutant backgrounds (Figure 4H; mutant + N-term). As a control, we demonstrate that neuronal overexpression (in a wild-type background) of either full-length Futsch or the N-terminal MAP1B homology domain of Futsch do not alter bouton number and do not affect the organization of synaptic microtubules (bouton numbers: full-length overexpression in wild-type background = 69.8 ± 3.2 and N-terminal overexpression in a wild-type background = 71.3 ± 3.0). There is, however, a slight reduction in average bouton size due to Futsch overexpression (Figure 4H; see also legend). We were able to drive overexpression of full-length Futsch in these experiments (despite not having a full-length cDNA) by taking advantage of a P(UAS) transposable element present in the 5′ regulatory region of *futsch* that can initiate *futsch* overexpression in the presence of a tissue-specific source of GAL4 (see Hummel et al., 2000). Thus, the N-terminal, predicted microtubule-binding domain of *futsch* is sufficient to partially rescue bouton number and bouton size in the *futsch* mutant backgrounds.

In addition to rescuing bouton number and bouton size, overexpression of the N-terminal domain of Futsch in the *futsch* mutant background partially rescues the organization and localization of microtubules within the mutant nerve terminal. Microtubules, while still having a punctate appearance, now localize to the periphery of the bouton rather than uniformly filling the volume of the bouton (ascertained with both 22C10 and antitubulin staining; compare Figure 4D1 with 4C1, 4G1, and 3A). We conclude that *futsch* is necessary for microtubule organization at the nerve terminal and that the N-terminal predicted MAP1B homology domain participates in this process. Furthermore, these data suggest that the correct organization of microtubules within the nerve terminal is necessary for the normal growth of synaptic boutons and for the normal addition of synaptic boutons to the synapse during development.

Microtubule Loops Persist throughout Development

A remarkable feature of microtubule organization at the nerve terminal is the formation of loop structures within select synaptic boutons. A small number of microtubule loops appear periodically along the nerve terminal. We observe that these intraterminal loops are closer together the further out they are along a chain of boutons. The average interloop distance in the proximal half of the nerve terminal (closer to the site of innervation) is 12.1 μm, and this decreases to 4.4 μm in the distal half of the nerve terminal. In addition, examination of microtubule loops at the second instar synapse (~2 days earlier in development) reveals that loops are on average closer together and that the loops are composed of a narrower gauge filament of Futsch (data not shown). This is consistent with loops forming during synaptic growth and then becoming stabilized structures within the nerve terminal. As the nerve terminal grows, more cytoskeleton is predicted to be added to

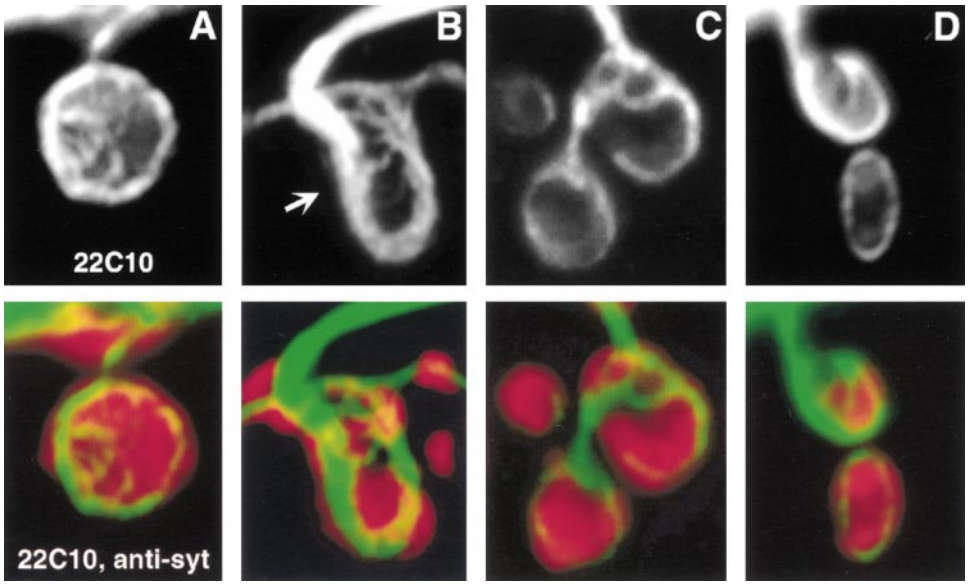

Figure 6. Predicted Progress of Synaptic Bouton Division

A series of different synaptic boutons (A–D) predicted to be at progressive stages of bouton division are shown from left to right. Each bouton is double stained for mAb 22C10 (top panel) and antisynaptotagmin (bottom panel showing the merged image with 22C10 in green and synaptotagmin in red). An arrow in (B) shows the predicted site of bouton cleavage during division and indicates the strands of Futsch-positive cytoskeleton that extend across the bouton at this point.

the synapse, and the gauge within the loops will be increased. In addition, boutons that are formed early in development will be separated by larger distances due to the expansion of the synapse with the growth of the muscle (Zito et al., 1999). Thus, loops formed early in development will be present in the proximal half of the NMJ and are predicted to be separated by larger distances, as observed.

Microtubules within Loops Do Not Rejoin the Major Cytoskeletal Core

An analysis of loop morphology demonstrates that microtubules within a loop do not rejoin the major cytoskeletal strand within the nerve terminal (Figure 5). We measured the diameter of the Futsch immunoreactivity 0.5 μm before and 0.5 μm after loop structures. We compared these measurements with diameters taken at two points separated by 4 μm (larger than the average diameter of a loop) at various positions along the nerve terminal without an interposed loop. Diameter measurements were taken after deconvolution of the nerve-terminal staining to reduce error associated with out-of-plane fluorescence scatter. The diameter of the main shaft of Futsch immunoreactivity is significantly reduced at the distal side of a loop compared to the proximal side (Figure 5C), whereas there is no change in the diameter of Futsch immunoreactivity over a similar distance of nerve terminal without an interposed loop. One essential role for Futsch as a microtubule-associated protein (MAP) could be to stabilize the microtubules at the free end of such a loop. The disruption of microtubule organization and loop formation in the *futsch* mutations supports this hypothesis.

Synaptic Microtubule Loops Identify Sites of Bouton Division

Live visualization of *Drosophila* neuromuscular synapses demonstrates that synaptic bouton division is a mechanism for bouton addition and branchpoint addition to the NMJ during development (Zito et al., 1999). This process is termed division as opposed to spouting because previously existing active zones are partitioned between newly formed boutons (Zito et al., 1999). Boutons that are predicted to be undergoing division can be identified by an irregular, hourglass-like shape (Zito et al., 1999). Examination of such bouton profiles demonstrates that these boutons not only contain microtubule loops, but these loops appear to be undergoing rearrangement (Figure 6). While dynamic rearrangement can only be proven by in vivo live observation, the irregular and highly variable branched microtubule structure is suggestive of an active process.

Examination of Futsch staining within numerous putative dividing boutons suggests a sequence for the process of bouton division (Figure 6). At the earliest stages of division, Futsch strands reach across the center of a loop within a bouton (Figure 6A). The strands of Futsch become more elaborate within boutons that have an hourglass-like shape, indicative of boutons that are midway through the process of division (Figure 6B). In many cases, strands of Futsch protein cross the middle of the dividing bouton precisely at the site where cleavage is predicted (Figure 6B, arrow). At the final stages of bouton division, two adjacent loops are produced in the neighboring newly divided boutons by the division of the original loop (Figures 6C and 6D). As the synapse grows, these new adjacent loops stabilize and later separate from one another as the synapse expands on the

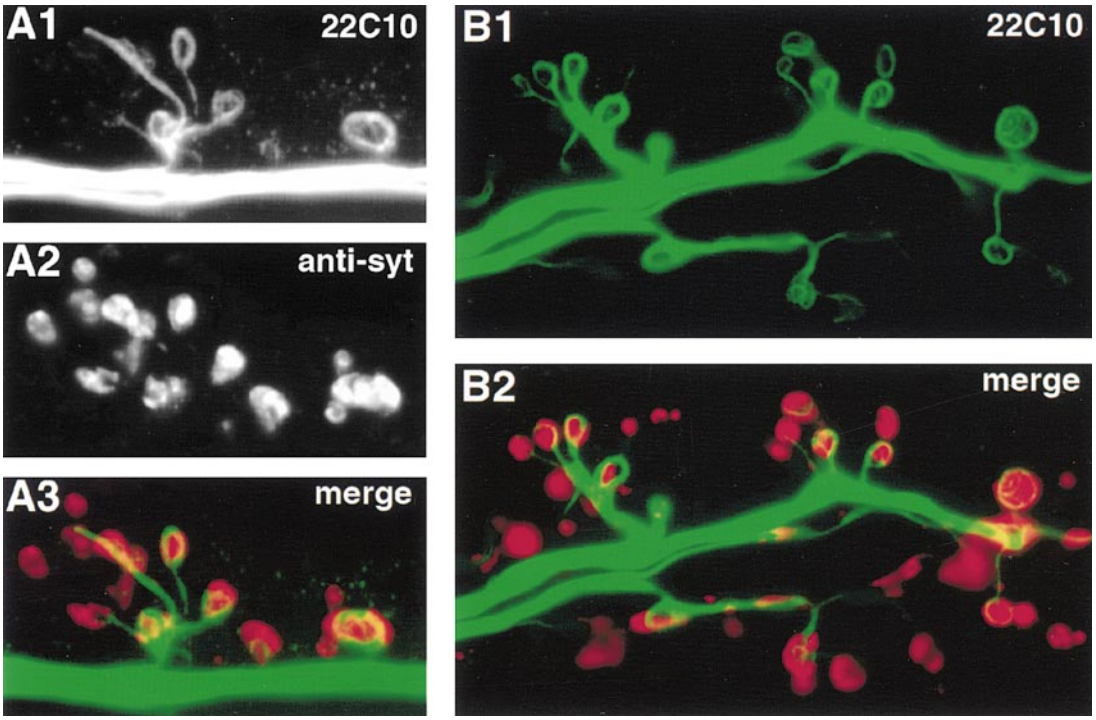

Figure 7. The Number of Presynaptic Futsch-Positive Loops Are Increased at Synapses Overexpressing *flexin* in All Muscle

(A) A synapse at muscles 6 and 7 double stained for mAb 22C10 (A1), antisynaptotagmin (A2), and the merged image showing the increase in loop number due to *flexin* overexpression.

(B) A synapse at muscles 6 and 7 showing a dramatic increase in Futsch loops due to postsynaptic *flexin* overexpression [(B1) mAb 22C10; (B2) merged image with antisynaptotagmin].

muscle surface, generating the stereotyped periodicity of loops within the synapse.

Interestingly, microtubule loops are always observed to lie in the same plane as the muscle fiber surface. If Futsch is involved in the process of bouton division, then the plane of the microtubule loop may also determine the plane of bouton division. This would prevent bouton division from occurring into the volume of the muscle fiber, which is never observed at the wild-type synapse.

Increased Synaptic Loop Formation Correlates with Increased Nerve-Terminal Branching

To support the conclusion that bouton division occurs at microtubule-based loops and is a mechanism of synaptic growth, we have taken advantage of a genetic background that increases the number of microtubule loops at the synapse. *flexin* is a novel *Drosophila* muscle protein (N. N. and G. W. D., unpublished data). Overexpression of *flexin* in muscle during postembryonic development causes a dramatic increase in nerve-terminal branching (Figure 7; N. N. and G. W. D., unpublished data). There is a two-fold increase in the occurrence of microtubule loops at *flexin* overexpressing synapses (Figure 7; 50% $\pm$ 4% of boutons contain a loop at *flexin* overexpressing synapses as compared to 22% $\pm$ 6% at wild-type synapses). This correlates with an approximate two-fold increase in nerve-terminal branch formation (N. N. and G. W. D., unpublished data). Thus, *flexin* appears to act as a muscle-derived signal to increase nerve-terminal branching. *flexin*-induced branching is correlated with increased organization of presynaptic microtubule loop structures.

Since Futsch is expected to act cell autonomously, elevated branching induced by *flexin* overexpression in muscle ought to be suppressed in a *futsch* mutant background. This was confirmed by the demonstration that muscle overexpression of *flexin* does not alter the *futsch*^{N94} mutant phenotype (overexpression of *flexin* being driven by the strong muscle promoter *24B-GAL4* [Davis et al., 1997]). There remains a reduction in bouton number (31.6 $\pm$ 4.1 boutons per synapse compared to wild type = 64.8 $\pm$ 4.1) and an increase in the average bouton size (26.6 μm^2 $\pm$ 6.6 compared to wild type = 9.3 μm^2) in *futsch*^{N94}*; flexin/24B-GAL4* larvae. Thus, normal *futsch* expression is necessary for the increased loop formation and increased branching observed when *flexin* is overexpressed in muscle.

Discussion

We have analyzed the role of a novel *Drosophila* gene, *futsch*, at the larval neuromuscular synapse. We demonstrate that *futsch* is necessary for the organization of microtubules within the nerve terminal. We further demonstrate that *futsch* is necessary for normal synaptic development, implicating a Futsch-dependent regulation of the microtubule cytoskeleton in this processes. Futsch may be particularly important for regulating the formation and stability of microtubule loops within synaptic boutons. Analysis of loop morphology and apparent loop dynamics suggests that rearrangement of these

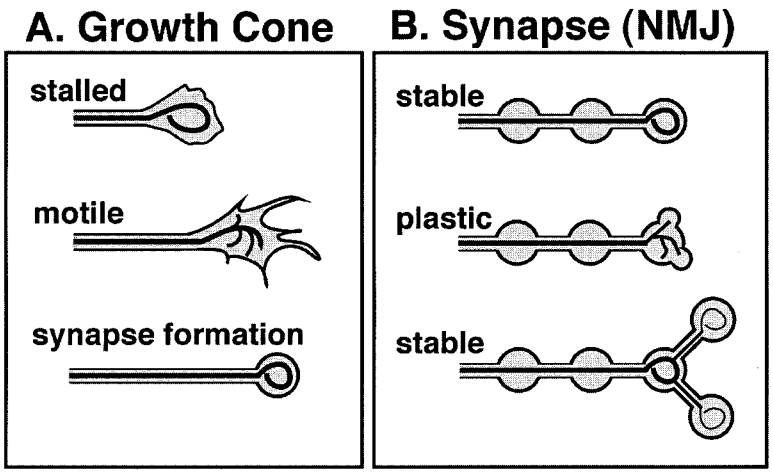

Figure 8. Microtubule Loop Specializations Implicate Common Growth Mechanisms at the Growth Cone and the End-Terminal Synaptic Bouton

(A) Regulated formation and disruption of microtubule loops correlates with growth cone motility (Dent et al., 1999). Microtubules within a stalled growth cone acquire a loop conformation. Resumed growth cone motility correlates with disruption of the loop conformation. Synapse formation, the transition of a motile growth cone to a stable synaptic contact, is once again correlated with the acquisition of a microtubule loop conformation within the newly formed synapse.

(B) At the developing *Drosophila* NMJ, the formation and reorganization of synaptic microtubule loops correlates with the division of select synaptic boutons. Bouton division (plastic) is correlated with the reorganization of microtubule loops. This bouton division is capable of branchpoint generation within the synapse. Microtubule loops are reestablished in the newly formed synaptic boutons.

microtubule-based loops is a critical component of the process of bouton division and for subsequent nerve-terminal growth and branching. We present a model in which Futsch participates in the regulation of synaptic growth by controlling the formation and rearrangement of microtubule-based loops that are present within a small subset of the synaptic boutons within each synapse (Figure 8). The presence of similar microtubule loops within growth cones, implicated in the process of growth cone motility, suggests a fundamental similarity between the mechanisms of synaptic growth and the mechanisms of growth cone dynamics.

A Model for Synaptic Growth Requiring Regulated Microtubule Loop Architecture

Our data indicate that the subsynaptic microtubule loops, identified by Futsch and tubulin immunoreactivity, are sites of bouton division within the neuromuscular synapse. Loops occur at stereotypic locations that are, or once were, sites of active bouton division including branchpoints and terminal boutons (Zito et al., 1999). In addition, examination of numerous putative dividing bouton profiles supports the conclusion that there is a progressive alteration in the microtubule-based loop architecture that is involved in the process of bouton division (Figure 6). Further genetic analysis, described below, supports this model. Ultimately, however, this model will have to be addressed by live, in vivo, visualization of synaptic microtubules during synaptic growth.

Genetic analysis of *futsch* function demonstrates that both microtubule organization and bouton division require wild-type Futsch. We observe fewer and larger boutons as well as impaired microtubule organization in *futsch* mutants. By analogy with cell division, this is the expected phenotype if bouton division were impaired. Genetic rescue experiments indicate that *futsch* can drive the processes of microtubule organization. Bouton size and number as well as microtubule organization are partially rescued by overexpression of the N-terminal MAP1B homology domain of *futsch*.

Further genetic analysis indicates that bouton division and subsequent nerve-terminal branching can be promoted by exogenous factors but require wild-type Futsch. There is a remarkable correlation between increased branching due to postsynaptic *flexin* overexpression and an increase in the number of presynaptic microtubule loops. Since the division of preexisting boutons occurs at loop-bearing boutons and since bouton division can generate nerve-terminal branching, our data present a correlation between increased loop formation and increased bouton division. Both elevated loop formation and increased branching require wild-type *futsch*, since *flexin* overexpression does not alter the *futsch* mutant phenotype. Although Futsch-dependent regulation of microtubule architecture predicts sites of apparent bouton division and appears necessary for this process, it remains to be determined whether microtubule rearrangement can drive this process.

Our hypotheses concerning the role of synaptic microtubule loops during bouton division is supported by analysis of similar structures observed within the growth cones of neurons in cell culture. Nearly identical microtubule loops (observed by injection of fluorescently labeled tubulin into cultured neurons) are observed within growth cones that have paused during their migration (Tsui et al., 1984; Tanaka and Kirschner, 1991; Dent et al., 1999). Resumed growth cone motility correlates with the disruption of the loop structure into fan-like conformations (Dent et al., 1999). Thus, highly organized loops within growth cones and within synaptic boutons are correlated with stability or lack of change, and the disruption of these loops is associated with motility and plasticity. Therefore, a switch from a stable mode to the active process of bouton division could be controlled by the regulated destabilization of microtubule loops (Figure 8).

A Molecular Switch for the Initiation of Morphological Synaptic Plasticity

It is likely that the dynamics of microtubule loops are controlled by a MAP. The small diameter of microtubule loops observed in growth cones and at the *Drosophila*

synapse indicates that a MAP is necessary to hold the microtubules in such a conformation. The predicted force necessary to bend polymerized tubulin into a loop with a diameter of ~3 μm is greater that the predicted buckling force of a microtubule (Gittes et al., 1993; Dogterom and Yurke, 1997). That vertebrate MAP1B may be involved in microtubule loop formation is supported by the demonstration that MAP1B overexpression in vitro induces the formation of wavy microtubule conformations (Pedrotti et al., 1996; Togel et al., 1998). Vertebrate MAPs including MAP1B are regulated by phosphorylation (Gordon-Weeks, 1997). Thus, phosphorylation could represent a switch capable of inducing rapid changes in microtubule loop conformation within a growth cone or synaptic bouton.

In vertebrates, phosphorylated MAP1B is enriched in growth cones (Bloom et al., 1985; Mansfield et al., 1991; Gordon-Weeks et al., 1993). The phosphorylation-dependent regulation of MAP1B and the subsequent effects on microtubule function are complex. Phosphorylation by casein kinase II appears to increase the affinity of MAP1B for microtubules (Aletta et al., 1988; Brugg and Matus, 1988; Diaz-Nido et al., 1988). Phosphorylation of MAP1B by glycogen synthase kinase 3-β (GSK3β) appears to maintain microtubules in a state of dynamic instability that is considered necessary for growth cone motility and migration (Goold et al., 1999; see review by Tanaka and Kirschner, 1995). It has been suggested that phosphorylation of MAP1B by GSK3β could act as a molecular switch to confer dynamic instability to microtubules, thereby promoting growth cone dynamics (Goold et al., 1999). In one model, phosphorylated Futsch could promote bouton division by promoting the dynamic instability of the microtubules within synaptic loops. Dephosphorylation of Futsch could decrease microtubule dynamics, promote loop formation, and switch synaptic boutons into a stable mode. If phosphorylation of Futsch is regulated by activity-dependent signaling, then the phosphorylation of Futsch could act as a permissive switch for activity-dependent plasticity at specific subsynaptic locations.

MAPs, Bouton Division, and Activity-Dependent Synaptic Plasticity

Recent results from studies of synaptic plasticity in the vertebrate brain indicate that the sprouting of new dendritic spines may be correlated with the consolidation of long-term synaptic plasticity (Engert and Bonhoeffer, 1999; Toni et al., 1999). Interestingly, MAP1B is enriched in areas of the vertebrate brain that show substantial activity-dependent synaptic plasticity (Caceres et al., 1986; Muller et al., 1994). Cytoskeletal rings have been observed in similar areas of the brain and in vertebrate hippocampal cell culture (Novotny, 1979; Shaw et al., 1985). We speculate that a MAP regulation of microtubule loops may participate in the process of synaptic morphological change within the vertebrate central nervous system during activity-dependent plasticity.

Conclusion

It has been hypothesized that the cellular mechanisms of growth cone motility and axon guidance are conserved during synapse elaboration and activity-dependent plasticity. However, morphological specializations that resemble the growth cone have not been observed at developing or plastic synapses (Zito et al., 1999). Data presented here and in Hummel et al. (2000) implicate a common mechanism in the control of growth cone motility and morphological synaptic plasticity. *Drosophila futsch* is essential for both axon elongation and synaptic growth. Futsch is implicated in the regulation of microtubule dynamics through the formation of microtubule loop structures at the synapse. Nearly identical microtubule structures have been previously demonstrated to regulate growth cone morphology and motility (Dent et al., 1999). The control of microtubule organization by MAPs may represent a common mechanism for regulated growth cone motility as well as synaptic growth and plasticity.

Experimental Procedures

Fly Stocks

Flies were raised on standard food at 25°C. The following strains were used for these studies: Canton S and w118 (wild type), *futsch^{N94}*, *futsch^{K68}*, *UAS-Nterm-Futsch/Cyo*, ep(X)1419, *UAS-tau-GFP*, and *flexin*. *futsch^{N94}* and *futsch^{K68}* are EMS-induced alleles of the *futsch* gene (Hummel et al., 2000). ep(X)1419 is a P(EP) element insertion upstream of the *futsch* gene capable of driving expression of the predicted full-length *futsch* transcript (Hummel et al., 2000; stock provided by Berkeley Drosophila Genome Center). *UAS-Nterminal-Futsch* corresponds to the genomic DNA representing the N-terminal 571 amino acids of *futsch* cloned into the pUAST vector as described (Hummel et al., 2000). *elaV-GAL4* and *24B-GAL4* are GAL4 lines that drive expression in all neurons and all muscle, respectively (Davis et al., 1997).

Overexpression of full-length *futsch* in the motoneuron was achieved by crossing ep(X)1419 by *elaV-GAL4*. Overexpression of the N-terminal region of *futsch* was achieved by crossing *UAS-Nterminal-Futsch/Cyo-GFP* by *elaV-GAL4* and analyzing non-GFP-positive larvae. For rescue of *futsch^{N94}* and *futsch^{K68}*, *UAS-Nterminal-Futsch; elaV-GAL4/SM6-TM6b* males were crossed to either *futsch^{N94}/futsch^{N94}* or *futsch^{N94}/futsch^{K68}* females. *futsch^{N94};UAS-Nterminal-Futsch/+*; *elaV-GAL4/+* or *futsch^{K68}; UAS-Nterminal-Futsch/+*; *elaV-GAL4/+* third instar larval males were identified as non-Tubby larvae lacking the SM6-TM6b-fused second-third chromosome balancer. Overexpression of *flexin* in postsynaptic muscle in the *futsch* mutant background was achieved by crossing *futsch^{N94}*; P(EP)*flexin* by *futsch^{N94}; 24B-GAL4*. All larvae were double stained with anti-syt to characterize synapse morphology and mAb 22C10 was used as an independent confirmation of the *futsch* genetic background.

Light Microscopy

Larval dissections and antibody staining were done as previously described (Schuster et al., 1996). Affinity-purified Dap160 polyclonal antibody (Roos and Kelly, 1999) was used at a concentration of 1:200; synaptotagmin antibody (Littleton et al., 1993) was used at a concentration of 1:1500; monoclonal antibody 22C10 (Developmental Studies Hybridoma Bank, University of Iowa) was used at a concentration of 1:50; α-tubulin monoclonal antibody (Sigma) was used at a concentration of 1:500. Fluorescent secondary antibodies (ICN/Cappel) were used at a concentration of 1:200. Direct conjugation of mAb 22C10 was achieved with 1 mg of antibody, diluted to 0.5 ml with PBS and conjugated with Alexa488 (Alexa488 Protein Labeling kit, Molecular Probes) as per the manufacturer's protocol. Images were acquired on a Delta-Vision workstation and processed with Delta-Vision deconvolution algorithms. For Figure 2, the deconvolved image was reconstructed in three dimensions using the volume viewer tool in the Delta-Vision software. Diameter of Futsch filaments were measured 0.5 μm before and after Futsch-positive loops. Control measurements were made on a 4 μm segment 2–3

μm upstream of the same loop. For each experimental genotype, between 30–50 segments in 10–20 animals were examined.

Acknowledgments

We would like to thank Regis Kelly for support and advice throughout this project. We also thank Pat O'Farrell for the use of the DeltaVision confocal microscope and Tony Shermoen for technical assistance with the confocal microscopy. We also thank Peter Clyne, Julia Kantor, Kurt Marek, and Suzanne Paradis for critical evaluation of a previous version of this manuscript. Finally, we thank Sarah Rice, Ron Vale, and Dyche Mullins for reagents, advice, and encouragement. Work was supported by a Burroughs Welcome Young Investigator Award, Merck Scholar Award, seed money, and a Young Investigator grant from the Sandler Foundation and NIH grant NS39313-01 (to G. W. D.). J. R. was supported by a NIH Postdoctoral Fellowship T32-CA 09270-23, and NIH grant NS15927 supported R. B. K.

Received January 27, 2000; revised April 18, 2000.

References

Aletta, J.M., Lewis, S.A., Cowan, N.J., and Greene, L.A. (1988). Nerve growth factor regulates both the phosphorylation and steady-state levels of microtubule-associated protein 1.2 (MAP1.2). J. Cell Biol. *106*, 1573–1581.

Bloom, G.S., Luca F.C., and Vallee, R.B. (1985). Microtubule-associated protein 1B: identification of a major component of the neuronal cytoskeleton. Proc. Natl. Acad. Sci. USA *82*, 5404–5408.

Brugg, B., and Matus, A. (1988). PC12 cells express juvenile microtubule-associated proteins during nerve growth factor-induced neurite outgrowth. J. Cell Biol. *107*, 643–650.

Caceres A., Banker, G.A., and Binder, L. (1986). Immunocytochemical localization of tubulin and microtubule-associated protein 2 during the development of hippocampal neurons in culture. J. Neurosci. *6*, 714–722.

Callahan, C.A., and Thomas, J.B. (1994). Tau-beta-galactosidase, an axon-targeted fusion protein. Proc. Natl. Acad. Sci. USA *91*, 5972–5976.

Casadio, A., Martin, K.C., Giustetto, M., Zhu, H., Chen, M., Bartsch, D., Bailey, C.H., and Kandel, E.R. (1999). A transient, neuron-wide form of CREB-mediated long-term facilitation can be stabilized at specific synapses by local protein synthesis. Cell *99*, 221–237.

Davis, G.W., Schuster, C.M., and Goodman, C.S. (1997). Genetic analysis of the mechanisms controlling target selection: target-derived Fasciclin II regulates the pattern of synapse formation. Neuron *19*, 561–573.

Dent, E.W., Callaway, J.L., Szebenyi, G., Baas, P.W., and Kalil, K. (1999). Reorganization and movement of microtubules in axonal growth cones and developing interstitial branches. J. Neurosci. *19*, 8894–8908.

Diaz-Nido, J., Serrano, L., Mendez, E., and Avila, J. (1988). A casein kinase II-related activity is involved in phosphorylation of microtubule-associated protein MAP1B during neuroblastoma cell differentiation. J. Cell Biol. *106*, 2057–2065.

Dogterom, M., and Yurke, B. (1997). Measurement of the force velocity relation for growing microtubules. Science *278*, 856–860.

Engert, F., and Bonhoeffer, T. (1999). Dendritic spine changes associated with hippocampal long-term synaptic plasticity. Nature *399*, 66–70.

Gallo, G., and Letourneau, P.C. (1999). Different contributions of microtubule dynamics and transport to the growth of axons and collateral sprouts. J. Neurosci. *15*, 3860–3873.

Gittes, F., Mickey, B., Nettleton, J., and Howard, J. (1993). Flexural rigidity of microtubules and actin filaments measured from thermal fluctuations in shape. J. Cell Biol. *120*, 923–934.

Goold, R.G., Owen, R., and Gordon-Weeks, P.R. (1999). Glycogen synthase kinase 3beta phosphorylation of microtubule-associated protein 1B regulates the stability of microtubules in growth cones. J. Cell Sci. *112*, 3373–3384.

Gordon-Weeks, P.R. (1997). MAPs in growth cones. In Brain Microtubule Proteins: Modifications in Alzheimer's Disease, J. Avila and K. Kosik, eds. (Harwood Academic Publishers), pp. 53–72.

Gordon-Weeks, P.R., Mansfield, S.G., Alberto, C., Johnstone, M., and Moya, F. (1993). A phosphorylation epitope on MAP 1B that is transiently expressed in growing axons in the developing rat nervous system. Eur. J. Neurosci. *5*, 1302–1311.

Grant, S.G., Karl, K.A., Kiebler, M.A., and Kandel, E.R. (1995). Focal adhesion kinase in the brain: novel subcellular localization and specific regulation by Fyn tyrosine kinase in mutant mice. Genes Dev. *9*, 1909–1921.

Halpain, S., Hipolito, A., and Saffer, L. (1998). Regulation of F-actin stability in dendritic spines by glutamate receptors and calcineurin. J. Neurosci. *18*, 9835–9844.

Hummel, T., Krukkert, K., and Klämbt, C. (2000). The *Drosophila* Futsch/22C10 protein is a MAP1B-like protein required for dendritic and axonal development. Neuron *26*, this issue, 357–370.

Ito, K., Sass, H., Urban, J., Hofbauer, A., and Schneuwly, S. (1997). GAL4 responsive UAS tau as a tool for studying the anatomy and development of the Drosophila central nervous system. Cell Tissue Res. *290*, 1–10.

Keshishian, H., Broadie, K., Chiba, A., and Bate, M. (1996). The drosophila neuromuscular junction: a model system for studying synaptic development and function. Annu. Rev. Neurosci. *19*, 545–575.

Littleton, J.T., Stern, M., Schulze, K., Perin, M., and Bellen, H.J. (1993). Mutational analysis of Drosophila synaptotagmin demonstrates its essential role in Ca(2+)-activated neurotransmitter release. Cell *74*, 1125–1134.

Luo, L., Jan, L.Y., and Jan, Y.N. (1997). Rho family GTP-binding proteins in growth cone signaling. Curr. Opin. Neurobiol. *7*, 81–86.

Mansfield, S.G., Diaz-Nido, J., Gordon-Weeks, P.R., and Avila, J. (1991). The distribution and phosphorylation of the microtubule-associated protein MAP 1B in growth cones. J. Neurocytol. *21*, 1007–1022.

Muller, R., Kindler, S., and Garner, C.C. (1994). The MAP1 family. In Microtubules, J.S. Hyams and C.W. Lloyd, eds. (New York: Wiley-Liss), pp. 141–151.

Novotny, G.E. (1979). Synaptic ring images after silver impregnation. Cell Tissue Res. *204*, 141–145.

Pedrotti, B., Francolini, M., Cotelli, F., and Islam, K. (1996). Modulation of microtubule shape in vitro by high molecular weight microtubule associated protein MAP1A, MAP1B, and MAP2. FEBS Lett. *384*, 147–150.

Rohatgi, R., Ma, L., Miki, H., Lopez, M., Kirchhausen, T., Takenawa, T., and Kirschner, M.W. (1999). The interaction between N-WASP and the Arp2/3 complex links Cdc42-dependent signals to actin assembly. Cell *97*, 221–231.

Roos, J., and Kelly, R.B. (1999). The endocytic machinery in nerve terminals surrounds sites of exocytosis. Curr. Biol. *9*, 1411–1414.

Schuster, C.M., Davis, G.W., Fetter, R.D., and Goodman, C.S. (1996). Genetic dissection of structural and functional components of synaptic plasticity. II. Fasciclin II controls presynaptic structural plasticity. Neuron *17*, 655–667.

Shaw, G., Banker, G.A., and Weber, K. (1985). An immunofluorescence study of neurofilament protein expression by developing hippocampal neurons in tissue culture. Eur. J. Cell Biol. *39*, 205–216.

Suter, D.M., and Forscher, P. (1998). An emerging link between cytoskeletal dynamics and cell adhesion molecules in growth cone guidance. Curr. Opin. Neurobiol. *8*, 106–116.

Tanaka, E.M., and Kirschner, M.W. (1991). Microtubule behavior in the growth cones of living neurons during axon elongation. J. Cell Biol. *115*, 345–363.

Tanaka, E., and Kirschner, M.W. (1995). The role of microtubules in growth cone turning at substrate boundaries. J. Cell Biol. *128*, 127–137.

Tanaka, E., and Sabry, J. (1995) . Making the connection: cytoskeletal rearrangements during growth cone guidance. Cell *83*, 171–176.

Tanaka, E., Ho, T., and Kirschner, M.W. (1995). The role of microtubule dynamics in growth cone motility and axonal growth. J. Cell Biol. *128*, 139–155.

Togel, M., Wiche, G., and Propst, F. (1998). Novel features of the light chain of microtubule associated protein MAP1B: microtubule stabilization, self-interaction, actin filament binding and regulation by the heavy chain. J. Cell Biol. *143*, 695–707.

Toni, N., Buchs, P.A., Nikonenko, I., Bron, C.R., and Muller, D. (1999). LTP promotes formation of multiple spine synapses between a single axon terminal and a dendrite. Nature *402*, 421–425.

Tsui, H.T., Kankford, K.L., Ris, H., and Klein, W.L. (1984). Novel organization of microtubules in cultured central nervous system neurons: formation of hairpin loops at ends of maturing neurites. J. Neurosci. *4*, 3002–3013.

Wills, Z., Bateman, J., Korey, C.A., Comer, A., and Van Vactor, D. (1999a). The tyrosine kinase Abl and its substrate enabled collaborate with the receptor phosphatase Dlar to control motor axon guidance. Neuron *22*, 301–312.

Wills, Z., Marr, L., Zinn, K., Goodman, C.S., and Van Vactor, D. (1999b). Profilin and the Abl tyrosine kinase are required for motor axon outgrowth in the *Drosophila* embryo. Neuron *22*, 291–299.

Zito, K., Parnas, D., Fetter, R.D., Isacoff, E.Y., and Goodman, C.S. (1999). Watching a synapse grow: noninvasive confocal imaging of synaptic growth in *Drosophila*. Neuron *22*, 719–729.